Available online at www.sciencedirect.com

jmr&t Journal of Materials Research and Technology

www.jmrt.com.br

Original Article

The effect of copper addition on the corrosion resistance of cast duplex stainless steel

Hillane Mirelle Lopes Ferreira de Lima[a,*], *Sérgio Souto Maior Tavares*[b], *Marcelo Martins*[c], *Walney Silva Araújo*[a]

[a] *Universidade Federal do Ceará – Departamento de Engenharia Metalúrgica e Materiais, Av. Mister Hull, s/n – Pici, Fortaleza, CE, Brazil*
[b] *Universidade Federal Fluminense – Departamento de Engenharia Mecânica, Rua Passo da Pátria, 156, Niterói, RJ, Brazil*
[c] *Centro Universitário Salesiano São Paulo, Engenharia Elétrica, Rua Dom Bosco 100, Santa Catarina, Americana, SP, Brazil*

ARTICLE INFO

Article history:
Received 17 August 2018
Accepted 13 January 2019
Available online 18 March 2019

Keywords:
Cast duplex stainless steel
Copper
Passive film
Pitting corrosion

ABSTRACT

In this study, the effects of the addition of 3.01% Cu on the corrosion behaviour of cast duplex stainless steel aged for 1 h at different temperatures between 450 and 600 °C was investigated by electrochemical tests in 0.6 M NaCl, 0.3 M H_2SO_4 and 0.6 M NaCl + 0.3 M H_2SO_4. A short ageing time increases the hardness and mechanical resistance of the Cu-containing steel by precipitation hardening. Potentiodynamic polarization and electrochemical impedance spectroscopy results show that the effect of Cu addition depends on the media studied. In addition, critical pitting temperature (CPT) measurements revealed that steel with 3.01% Cu has a lower pitting corrosion resistance. On the other hand, for both steels, the short time ageing caused a slight increase in CPT values.

1. Introduction

Duplex stainless steels (DSSs) have a two-phase structure comprising island-like austenite (γ phase, fcc) in a continuous ferrite matrix (α phase, bcc) [1–3]. The relationship between the two phases is usually about 50% (by volume fraction). Cast DSSs are used in cooling water pipes, valve bodies, pump casings and elbows of light water nuclear reactors due to their excellent characteristics, such as high strength, ductility, good weldability and excellent resistance to stress corrosion cracking [3–5]. The high resistance of stainless steels to corrosion is attributed to the dynamic properties of their passive films [6,7], which are influenced by many factors, such as the metal type, alloy composition, electrode potential, pH and electrolyte composition [6,8].

Nevertheless, if DSSs are exposed to a certain range of high temperature, the balance of alloying elements can be disturbed by precipitation of various secondary phases. In this way, these steels are prone to age hardening and embrittlement over a wide temperature range. The temperature range between 300 and 600 °C is characterized by the spinodal decomposition of ferrite into Cr-poor α and Cr-rich α′ domains. Other precipitation processes also occur depending on the actual chemical composition of the steel, the main two being

* *Corresponding author.*
E-mail: hillanemirelle@gmail.com (H.M. Lima).
https://doi.org/10.1016/j.jmrt.2019.01.018

Table 1 – Chemical composition for the DSSs (wt.%).

	C	Cr	Ni	Mn	Si	Mo	Cu	N	Fe
1B	0.043	25.64	4.51	0.68	0.80	2.01	**3.01**	0.21	Bal.
3A	0.025	24.59	5.61	0.78	0.91	2.02	–	0.17	Bal.

the spinodal decomposition of ferrite into Cr-rich α' and Cr-depleted α'' and the production of a Ni, Si, Cu, Mo-rich G-phase precipitate [9–12]. Some commercial duplex stainless steels contain 0.5–1.0 wt.% copper to improve corrosion resistance by reducing the corrosion rate in non-oxidizing environments, notably sulphuric acid [13–16]. The solubility of copper is relatively high in austenite (~4%) and low in ferrite (~0.2%) [17,18]. Ageing after solution treatment causes significant hardening by precipitation of fine copper precipitates (ε-phase). The small particles of this phase (<300 Å) contain up to 96 wt.% Cu [17]. Thus, a higher copper addition (≥2%) can also introduce precipitation hardening, as done in other types of stainless steel (ex.: 17-4PH martensitic steel). This strengthening mechanism is especially useful for cast components that cannot be thermomechanically treated to improve mechanical resistance. However, the effects of Cu addition on the localized corrosion performance of aged alloys in chloride media have not been clarified sufficiently and there is some controversy in the literature regarding stainless steel composition and experimental conditions (pH, temperature, chloride concentration, for example).

In this work, the electrochemical behaviour of two cast duplex stainless steels, ASTM A890/A 890M [19] grades 1B and 3A, were investigated. Grade 1B steel contains 3.01 wt.% Cu and grade 3A steel is Cu free. Different levels of hardness were produced by solution treatment and ageing at 450, 500, 550 and 600 °C for up to 1 h. The corrosion resistance was evaluated by electrochemical tests (critical pitting temperature, cyclic polarization and electrochemical impedance spectroscopy (EIS)) in 0.6 M NaCl, 0.3 M H_2SO_4 and 0.6 M NaCl + 0.3 M H_2SO_4 solutions. The effect of ageing on the corrosion behaviour of the steels was investigated by comparing the results of samples aged with those solution treated. Microstructural characterization was performed by optical and scanning electron microscopy (SEM). Specimens were observed after the corrosion tests.

2. Experimental

The two grades of cast DSS, ASTM A890/A 890M grades 1B and 3A [19], were provided by Sulzer Brazil S/A. The chemical compositions in Table 1 show that the main difference between the two steels is the copper content (3.01% in grade 1B). The pitting corrosion equivalent number (PREN), calculated by PREN = wt.% Cr + 3.3 wt.% Mo + 16 wt.% N [13] was 35.6 for grade 1B and 33.9 for grade 3A.

Samples of both steels were annealed (1100 °C for 1 h followed by water quenching). The objective of the solution annealing heat treatment before ageing was to obtain complete dissolution of the precipitates in the ferrite matrix and at the α/γ interfaces [20]. Then, samples were subjected to a range of isothermal heat treatment from 450 to 600 °C for 1 h. The heat treatment was performed in a muffle furnace.

Vickers hardness tests with a 10 kgf load were performed on each specimen to evaluate the effect of precipitation hardening in both steels.

Metallographic investigations were carried out using optical microscopy (OM). The specimens for microstructural observation were abraded with silicon carbide papers from 120 to 2000 grit. They were polished with several grades of diamond pastes, degreased with alcohol, washed with distilled water, dried with hot air and then, finally, microstructures were revealed using the Beraha reagent (20 mL HCl, 80 mL distilled water, and 1 g of potassium metabisulfide), which made the austenite phase light and the ferrite phase dark. Specimens were then obtained by OM.

The effects of Cu addition on the electrochemical corrosion behaviour were evaluated by analysing the cyclic polarization tests and EIS in naturally aerated 0.6 M NaCl, 0.3 M H_2SO_4 and 0.6 M NaCl + 0.3 M H_2SO_4 solutions. Pitting behaviour was studied using critical pitting temperature (CPT) tests. A conventional three-electrode electrochemical cell using a platinum (Pt) grid as the counter electrode, saturated KCl silver/silver chloride (Ag/AgCl) as the reference electrode and the working electrode was constructed using the steel samples embedded in epoxy resin. The working electrode area exposed to the test solution was approximately 0.5 cm^2. Before the electrochemical tests, the specimens were abraded with silicon carbide paper (up to 600 grit), degreased with alcohol, washed with distilled water and dried with hot air. In order to prevent the possibility of crevice corrosion during measurement, the interface between the sample and resin was coated with transparent lacquer. The tests were initiated after a nearly steady-state open circuit potential (OCP) was developed (60 min), in a potentiostat-galvanostat Autolab model PGSTAT302N. The cyclic polarization and EIS measurements were made at room temperature, 25.0 ± 0.2 °C. Each experiment was run at least three times, and the data showed good reproducibility.

In order to complete the study of the influence of Cu addition and ageing on pitting corrosion resistance of DSSs, CPT values were measured in 1 M NaCl solution using a potentiostatic polarization method [21]. The working electrode was polarized to 700 mV vs. Ag/AgCl (KCl sat.) and the temperature was increased at a rate of 1 °C min^{-1} until stable pitting had occurred starting from 25 °C. The current was measured against temperature, and the CPT was that corresponding to a current density of 100 μA cm^{-2}.

Cyclic polarization tests were performed by increasing the potential at a scan rate of 1.0 mV s^{-1} until a current of 1.0 mA was reached, at which point the scanning direction was then reversed. The surface of the specimen subject to polarization was observed just after the test by OM. Impedance spectra were obtained at the corrosion potential with a frequency

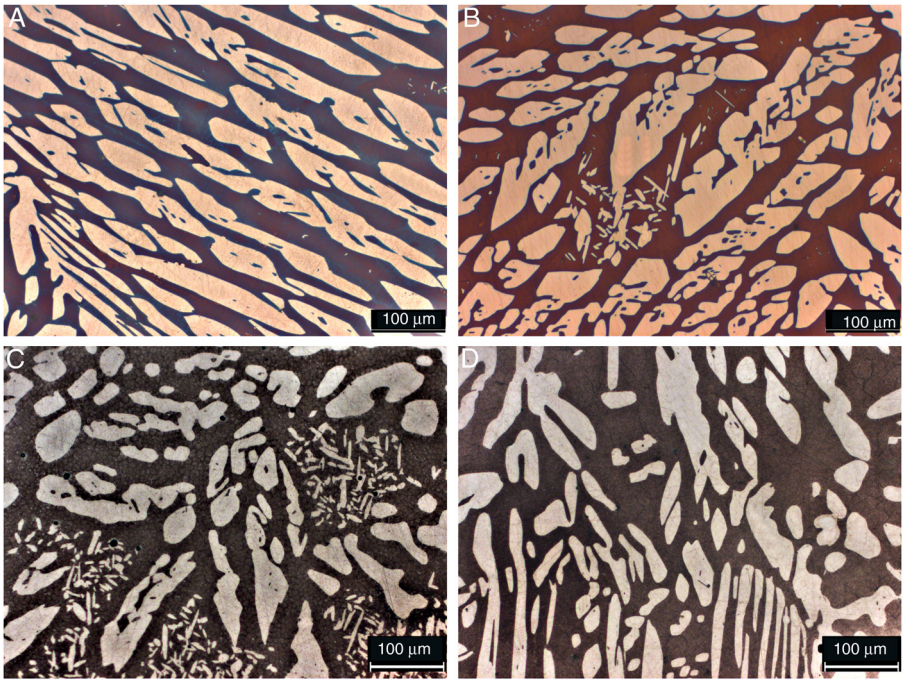

Fig. 1 – Optical micrographs of the microstructures of samples (A) 1B annealed, (B) 1B aged at 600 °C for 1 h, (C) 3A annealed and (D) 3A aged at 600 °C for 1 h.

range from 10 kHz to 2.5 mHz with a signal amplitude perturbation of 25 mV and 7 points/decade. Specimens were observed after the corrosion tests by OM and SEM.

3. Results and discussion

3.1. *Metallographic observations*

The microstructures of the solution-annealed materials consist of austenite islands (the brighter phase) embedded in a ferrite matrix (the darker phase) without apparent secondary phase precipitation. The nominal volume fractions of both ferrite (α) and austenite (γ) in all the samples, measured by quantitative OM, remained unchanged with ageing temperature and were close to 50%, the final value was the average of at least 12 measurements, indicating a good balance of both phases. Some previous studies [22–25] suggested that ageing DSSs in temperatures between 350 and 600 °C would cause spinodal decomposition of the ferrite into chromium-depleted (α″) and chromium-rich (α′) regions. In addition to spinodal decomposition, other precipitation processes would also occur depending on the chemical composition of the steel; the main one being the precipitation of ε(Cu), Ni, Si, Mo-rich G-phase. Thereby, as mentioned before, copper additions above 1% can lead to ε-phase precipitation. The grade 1B steel contained 3.10% Cu (Table 1), suggesting an extra-fine precipitate concentration [17,26]. However, there was no significant change in the microstructures of specimens after ageing between 450 and 600 °C for 1 h, as seen in Fig. 1. These results are in good agreement with the literature, which reports that microstructural changes in SDSS at low temperatures occur at the nanometric scale and are not visible by OM and/or SEM [9–12].

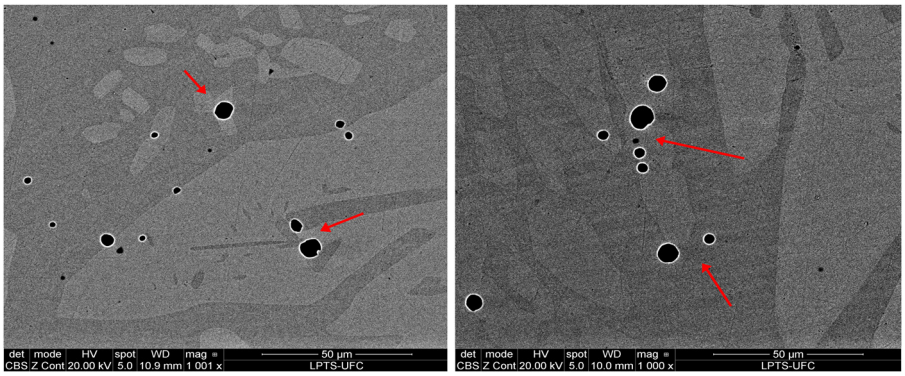

Fig. 2 – Back-scattered electron (BSE) images of the inclusions in the annealed sample: (A) 1B and (B) 3A.

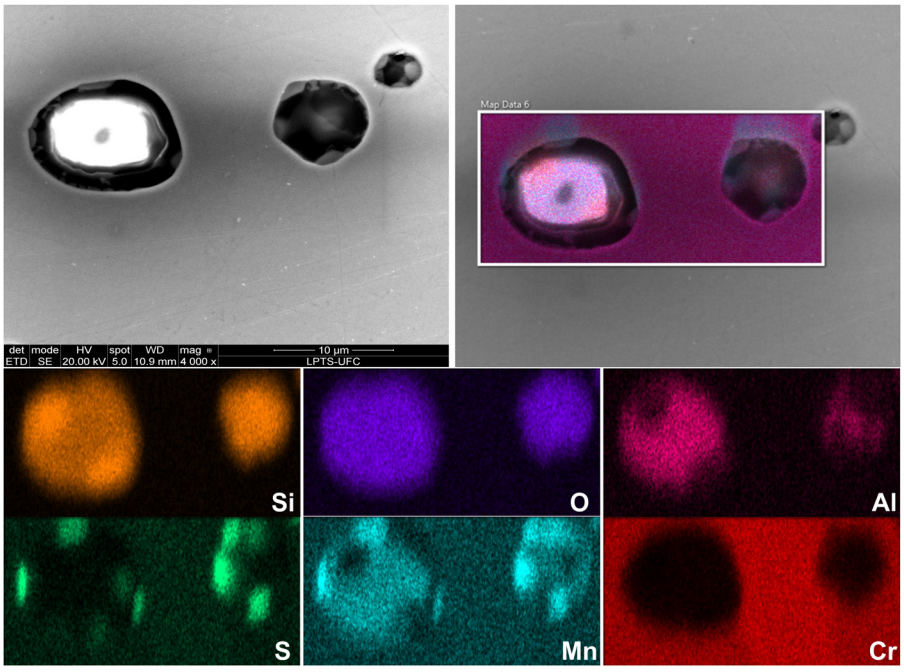

Fig. 3 – SEM–EDS analysis of inclusions in the 1B DSS annealed.

3.2. *Inclusions*

Fig. 2 shows back-scattered electron (BSE) images of the experimental alloys in which inclusions may be observed. The non-metallic inclusions are typically spherical and uniformly distributed in the material. The chemical composition of the inclusions (black spots in Fig. 2) was analyzed by SEM–EDS (Fig. 3). As presented in Fig. 3(c), the inclusions in the alloy were composed of complex Si, Al and Mn oxides and oxy-sulfides. The chemical compositions of inclusions in both aged steels were similar to those in the annealed condition. Such complex oxide inclusions are typical of cast DSSs and may act as sites of deleterious phase nucleation, such as the sigma phase in high-temperature exposition [27].

3.3. *Precipitation hardening effect*

After solution treatment, the hardness of 1B and 3A steels was 235 ± 4 HV10 and 245 ± 8 HV10, respectively, suggesting that Cu does not harden by solid solution. Table 2 shows the increase of hardness (ΔH) produced in each steel by ageing for 1 h in the 4 temperatures investigated. It is worth noting that these are not the peak hardness at each temperature. It is possible to observe that the hardness of 1B steel (Cu-alloyed specimens) is greater than 3A steel (Cu-free specimens). The higher ΔH observed in 1B steel is attributed to α' and ε(Cu) phase precipitation [17], which makes a difference in the short-term ageing in all temperatures studied. Between the aged samples, there is a decrease in ΔH values with increasing ageing temperature, which is more intense for Cu-alloyed specimens (1B). The lower hardness observed at 550 and 600 °C characterizes an overageing process. For longer-term ageing, it is expected that Cu-free 3A steel undergoes more pronounced hardening due to the spinodal decomposition of ferrite [3–5].

3.4. *Open potential circuit (OCP)*

The evolution of the OCP for 1B and 3A DSSs monitored versus time in 0.6 M NaCl, 0.3 M H_2SO_4 and 0.6 M NaCl + 0.3 M H_2SO_4 are shown in Fig. 4. A higher OCP value usually indicates a decrease in the electrochemical activity of the steel surface [26,28,29]. As a general tendency, the potential increased as soon as the samples were immersed in the electrolyte and then stabilized. Comparison of the 1B and 3A samples show that the OCP values obtained for the Cu-free specimens (3A) were always more negative, which is indicative of a more active corrosion surface when compared with the Cu-alloyed specimens (1B). This result could be related to a protective effect of Cu. Additionally, the OCP and the critical time for stabilization of the potential were different according to the immersion medium. The OCP of DSSs immersed in 0.6 M NaCl

Table 2 – Increase of hardness (ΔH) with ageing at 450, 500, 550 and 600 °C for 1 h.

Steel	450 °C/1 h	500 °C/1 h	550 °C/1 h	600 °C/1 h
1B	58 ± 10	38 ± 12	25 ± 9	11 ± 6
3A	34 ± 11	32 ± 9	11 ± 12	0 ± 6

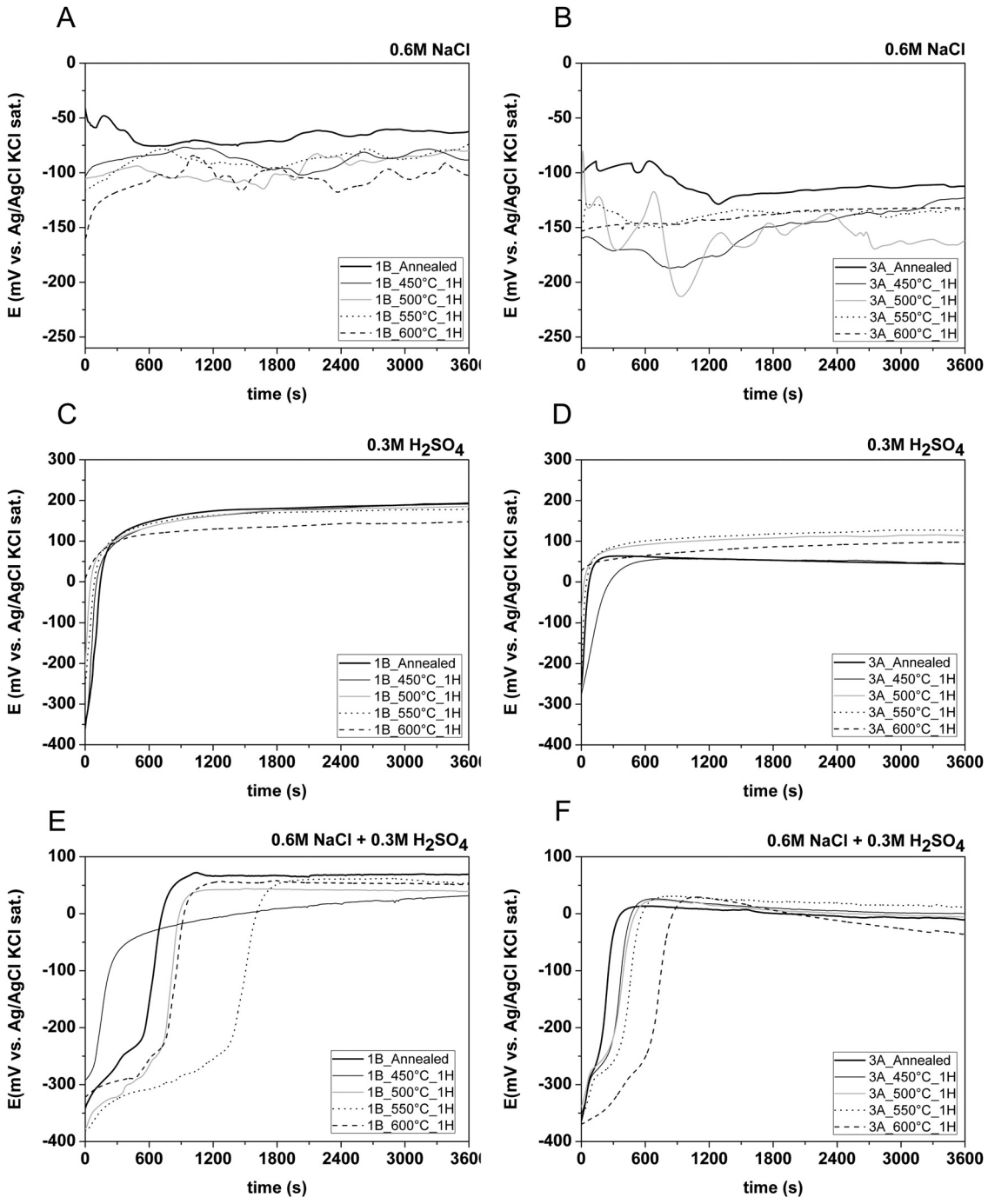

Fig. 4 – Typical evolution of open circuit potential with time of samples in (A), (B) 0.6 M NaCl; (C), (D) 0.3 M H_2SO_4; (E), (F) 0.6 M NaCl + 0.3 M H_2SO_4.

were more negative, which may indicate a more active corrosion surface when compared with the specimens immersed in an acidic medium. For samples immersed in 0.3 M H_2SO_4, the OCP value is negative at first, due to the dissolution of an air formed oxide film, and then increases towards a steady state value after few minutes. On the other hand, the samples immersed in 0.6 M NaCl + 0.3 M H_2SO_4 electrolyte took more time for stabilization of potential (about 1800 s). According to the OCP values, the addition of Cu to the DSSs composition was beneficial in all the mediums investigated.

3.5. *Potentiodynamic polarization behaviour*

The measurement of a steady-state anodic polarization curve over the wide potential range is usually a first step in studying passivity. The literature shows that the corrosion resistance of stainless steels is primarily attributed to passive film growth on its surface [29–31]. The changes and breakdown of the passive film directly affect the localized corrosion resistance, leading to pitting corrosion, crevice corrosion, intergranular corrosion and stress corrosion cracking. Therefore, understanding

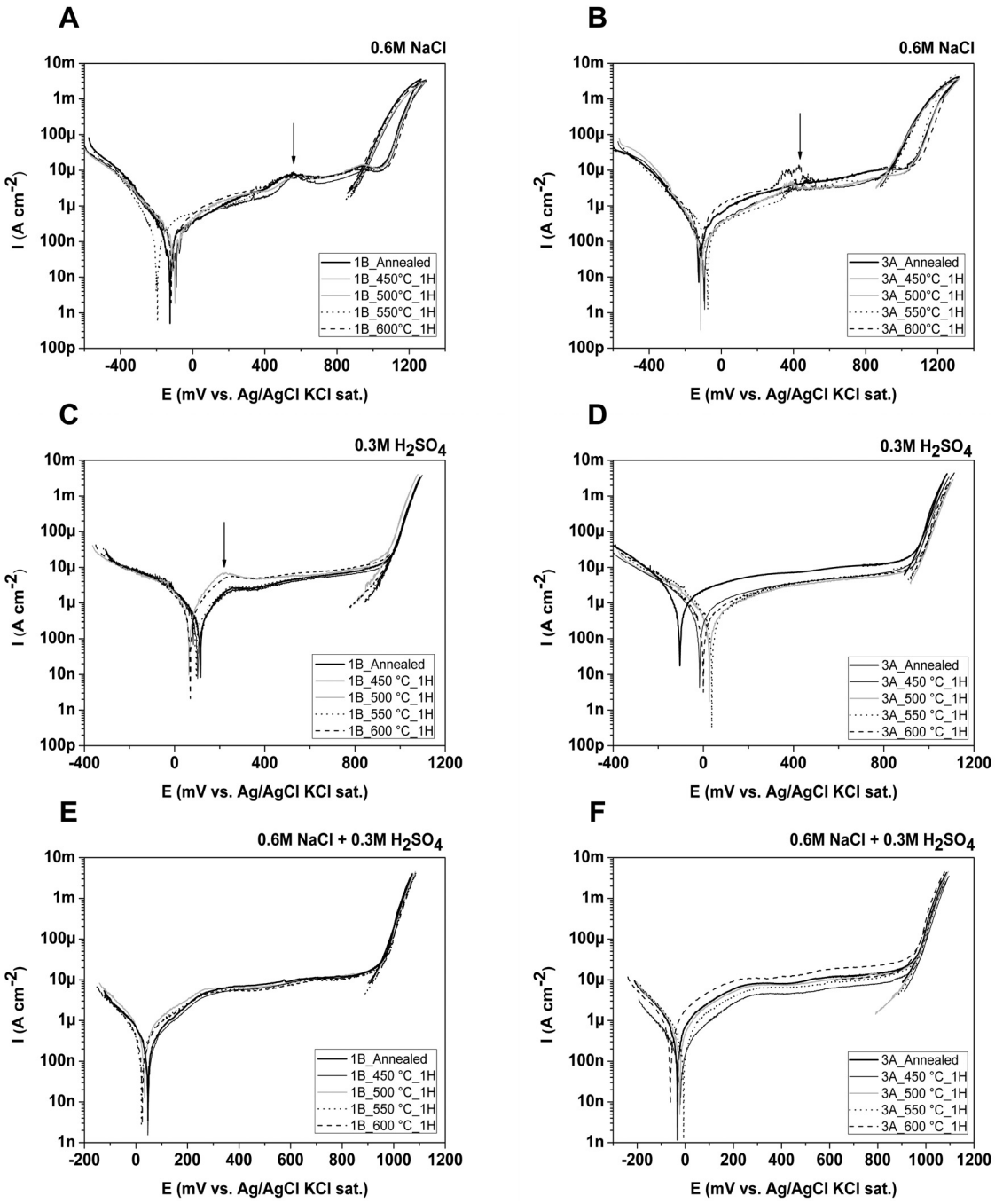

Fig. 5 – Cyclic polarization curve of samples in (A), (B) 0.6 M NaCl; (C), (D) 0.3 M H_2SO_4; (E), (F) 0.6 M NaCl + 0.3 M H_2SO_4.

the passivity properties is a key factor for the protection of stainless steels against localized corrosion attacks. One of the most common approaches to reducing localized corrosion-related failures involves the selection of a suitable alloy.

Fig. 5 shows the cyclic potentiodynamic polarization curves of the alloys under the different heat treatment conditions in 0.6 M NaCl, 0.3 M H_2SO_4 and 0.6 M NaCl + 0.3 M H_2SO_4 solutions at 25 °C. As can be seen, all the specimens are characterized by a very wide potential domain of passivity (between 0.2 and 1.0 V vs. Ag/AgCl) in all media studied. Samples annealed and aged presented a low current density, around a few $\mu A\,cm^{-2}$ at up to 1.0 V (vs. Ag/AgCl). An abrupt increase of current, for these samples, occurred in the potential range where oxygen evolution could already thermodynamically take place. At higher potentials, the oxygen anodic reaction seemed to participate in pitting nucleation through the formation of a triple interface between the metal, electrolyte and oxygen bubbles [32]. Therefore, the steep increase at ~1.0 V vs. Ag/AgCl for these samples is likely due but to the onset of oxygen evolution not to pitting corrosion.

Fig. 5(a, b) shows similar polarization characteristics for 1B and 3A samples in 0.6 M NaCl solution. The anodic polarization behaviour of both steels consists of active dissolution with no distinctive transition to passivation, passivity and a rapid increase of the current density. However, when the potential reaches the passivation state, a peak was detected at about 400 mV vs. Ag/AgCl in both materials (see the arrows in Fig. 5a, b). This anodic peak corresponds to the initiation of pitting corrosion and the repassivation of metastable pits [33,34]. It is worth noting that this peak was only observed in 0.6 M NaCl solution.

The polarization behaviour of the specimens immersed in 0.3 M H_2SO_4 (Fig. 5c, d) is somewhat different. The active–passive transition peak was only observed for the 1B DSSs (Cu-containing samples) within the studied potential range (see the arrow in Fig. 5c). In this way, although the corrosion potentials of 1B samples are more positive than those of 3A specimens, the Cu-free samples (3A) showed a wider passive region in comparison with Cu-containing samples (1B). Based on these results, the addition of Cu has a negative effect on the onset of passivation in 0.3 M H_2SO_4 solution. Additionally, for 3A steel (Fig. 5d), the curves of the aged samples were shifted towards more positive potential values. Moreover, the passivation current densities of the aged samples were lower than the solution treated sample. This trend may be an indication of the beneficial effect of short ageing times on the corrosion behaviour of the material.

A great difference in the electrochemical behaviour of samples immersed in 0.6 M NaCl + 0.3 M H_2SO_4 was observed. When the ageing temperature was extended to 600 °C, the passivation current density increased (from 5 $\mu A\,cm^{-2}$ for samples aged at 450 °C to 15 $\mu A\,cm^{-2}$ for samples aged at 600 °C), while all samples of grade 1B steel presented similar behaviour in the studied potential range (passivation current density about 8 $\mu A\,cm^{-2}$). This indicates that the stability of the passive film formed on 3A steel in acidic NaCl solution decreased with increasing ageing temperature, as shown in Fig. 5(f). It can also be inferred that the film formed on the Cu-free sample is less stable than that in Cu-containing specimens under the same heat treatment conditions in acidic NaCl solution.

Fig. 6 is the secondary electron image of the 1B sample aged at 450 °C after potentiodynamic polarization tests in 0.6 M NaCl + 0.3 M H_2SO_4. As can be seen, metastable pitting corrosion nucleates primarily at inclusions. Inclusions act as preferential sites for localized corrosion. However, based upon the polarization results, the presence of inclusions does not meaningfully influence the corrosion resistance of either steel in the mediums studied.

3.6. *Electrochemical impedance responses*

Electrochemical impedance spectra were measured at the OCP and the obtained impedance responses are presented in Nyquist and Bode formats for each of the different DSSs in 0.6 M NaCl (Fig. 7), 0.3 M H_2SO_4 (Fig. 8) and 0.6 M NaCl + 0.3 M H_2SO_4 (Fig. 9). For both 1B and 3A samples, the Nyquist plots have almost the same shape, where depressed capacitive semicircles cover almost all frequency regions. The capacitive arcs did not intersect the x-axis at any point in the frequency

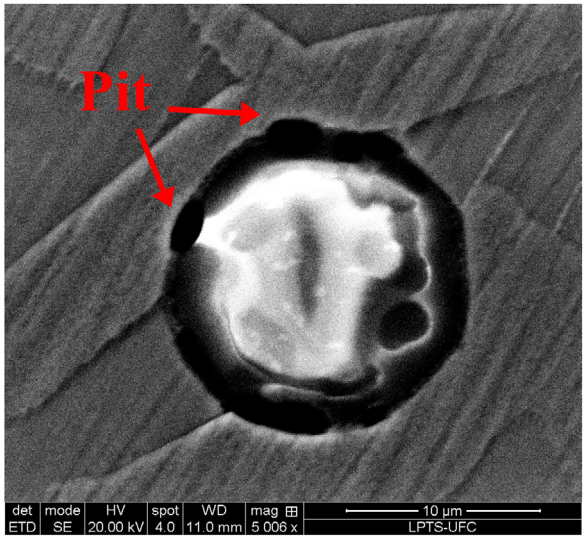

Fig. 6 – SEM analysis of inclusions in the 1B DSS aged at 450 °C after polarization tests in 0.6 M NaCl + 0.3 M H_2SO_4.

interval but rather consisted of partial circles of infinite radii. The appearance of the capacitive loop can be attributed to charge transfer processes associated with the effect of double layer capacitance, and its diameter is related to the charge transfer resistance (R_{ct}) at the metal/solution interface. The charge transfer resistance, R_{ct}, is commonly used as a measure of the resistance of a metal to corrosion damage. A high value of R_{ct} is associated with a high corrosion prevention capability; a low value of R_{ct} indicates potentially high corrosion activity. The data analysis was taken using NOVA version 1.11 software. The equivalent circuit proposed to fit the obtained experimental EIS data at OCP was R_s (CPE R_{ct}) [35,36], which comprises a solution resistance R_s, shorted by a constant phase element (CPE) that is placed in parallel with the charge transfer resistance, R_{ct}. An example of the shape of the spectra and quality of the fitting achieved is shown in Fig. 10. The others had similar behaviour and the measurements have errors in the range between 2 and 5%.

The equivalent circuit of one-time constant consists of the following elements: R_s (Ohm), used to simulate the value of the uncompensated solution resistance; R_{ct} (Ohm), used to simulate the charge transfer resistance; CPE, the value of the argument of the constant phase element (also referred to as a Y element); and n, the value of the exponent of the CPE. The CPE was introduced to characterize a "capacitance dispersion" related to the capacity of the material surface area with complex surface roughness, inhomogeneous reaction rates on a surface and non-uniform current distribution [33].

The magnitude of the charge transfer resistance (R_{ct}) was always higher for the Cu-containing specimens (1B) in each medium investigated. The low R_{ct} values for the specimens without Cu (3A) point towards their high corrosion susceptibilities. This indicates that Cu addition improves the corrosion resistance of the passive film. It was also observed that R_{ct} is always higher in 0.6 M NaCl than in acidic media for both materials (Table 3). The R_{ct} values decrease in the order of media NaCl > H_2SO_4 > (NaCl + H_2SO_4). This fact is sight surprising

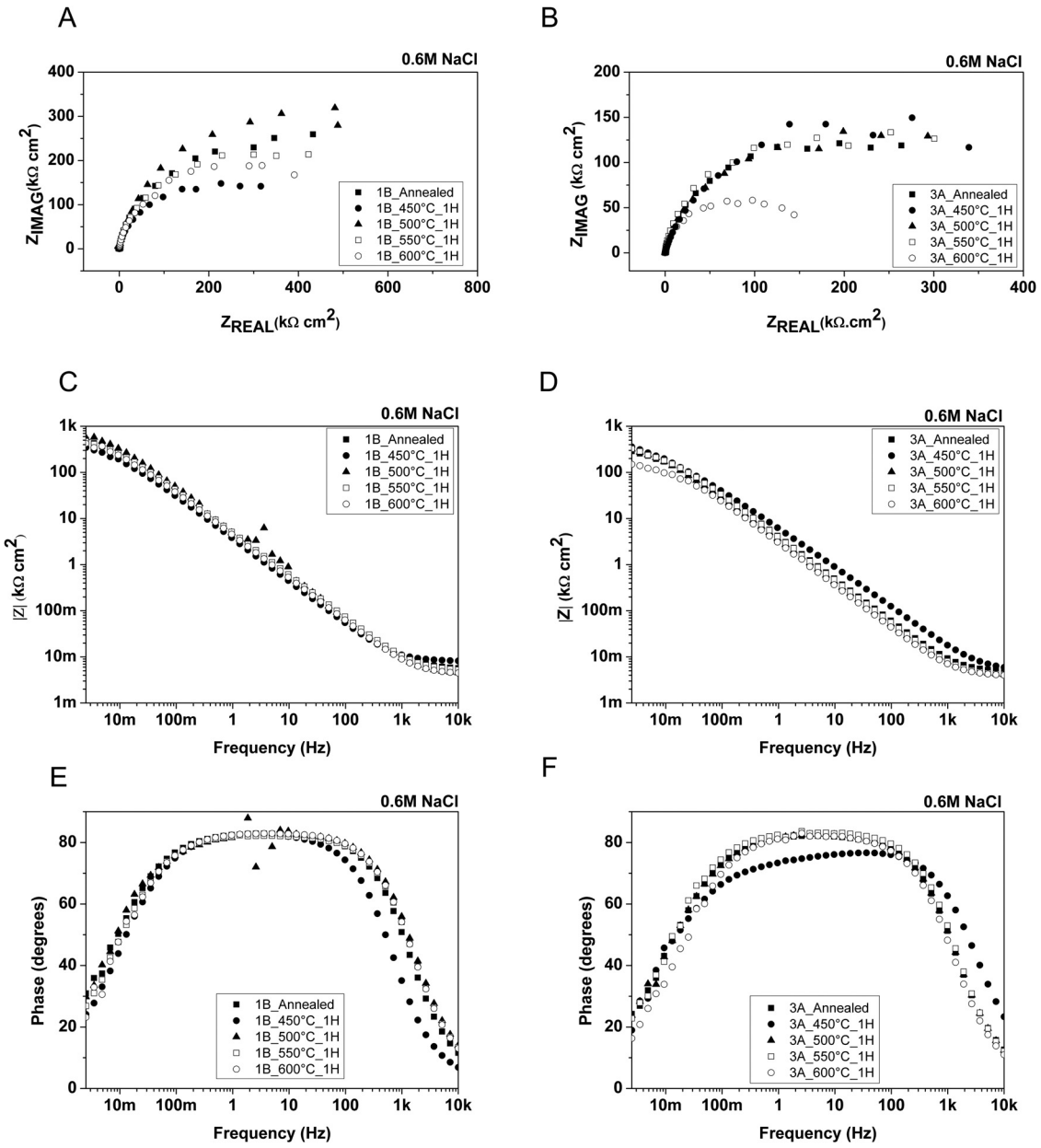

Fig. 7 – Bode and Nyquist plots for EIS data in 0.6 M NaCl of specimens: (A), (C), (D) 1B; (B), (D), (F) 3A.

at first because copper has been observed to considerably improve the general corrosion resistance of stainless steel in sulphuric media [15,34]. For the samples immersed in 0.3 M H_2SO_4 solution (Fig. 8), similar behaviour is observed for both steels; namely, the aged samples presented higher R_{ct} values than the reference sample in the solution treated condition. Again, this trend may be an indication of the beneficial effect of short ageing time on the corrosion behaviour of steel in this environment, which agrees with polarization measurements.

The phase angle vs. frequency reveals a peak at high to low frequencies, which represents the capacitive characters. A highly capacitive behaviour typical of passive materials is indicated from intermediate to low frequencies by phase angles approaching −90° over a wide range of frequencies in the Bode plots and suggests the formation of very stable surface films.

3.7. *Critical pitting temperature measurements*

Potentiostatic CPT measurements were carried out by the potentiostatic method described in ASTM G-150 [21]. Fig. 11 represents typical curves of current density versus temperature for specimens aged at different temperatures for 1 h during the CPT measurement by applying a 700 mV (Ag/AgCl) anodic potential and gradually increasing the temperature. The CPT corresponds to the temperature in which the current

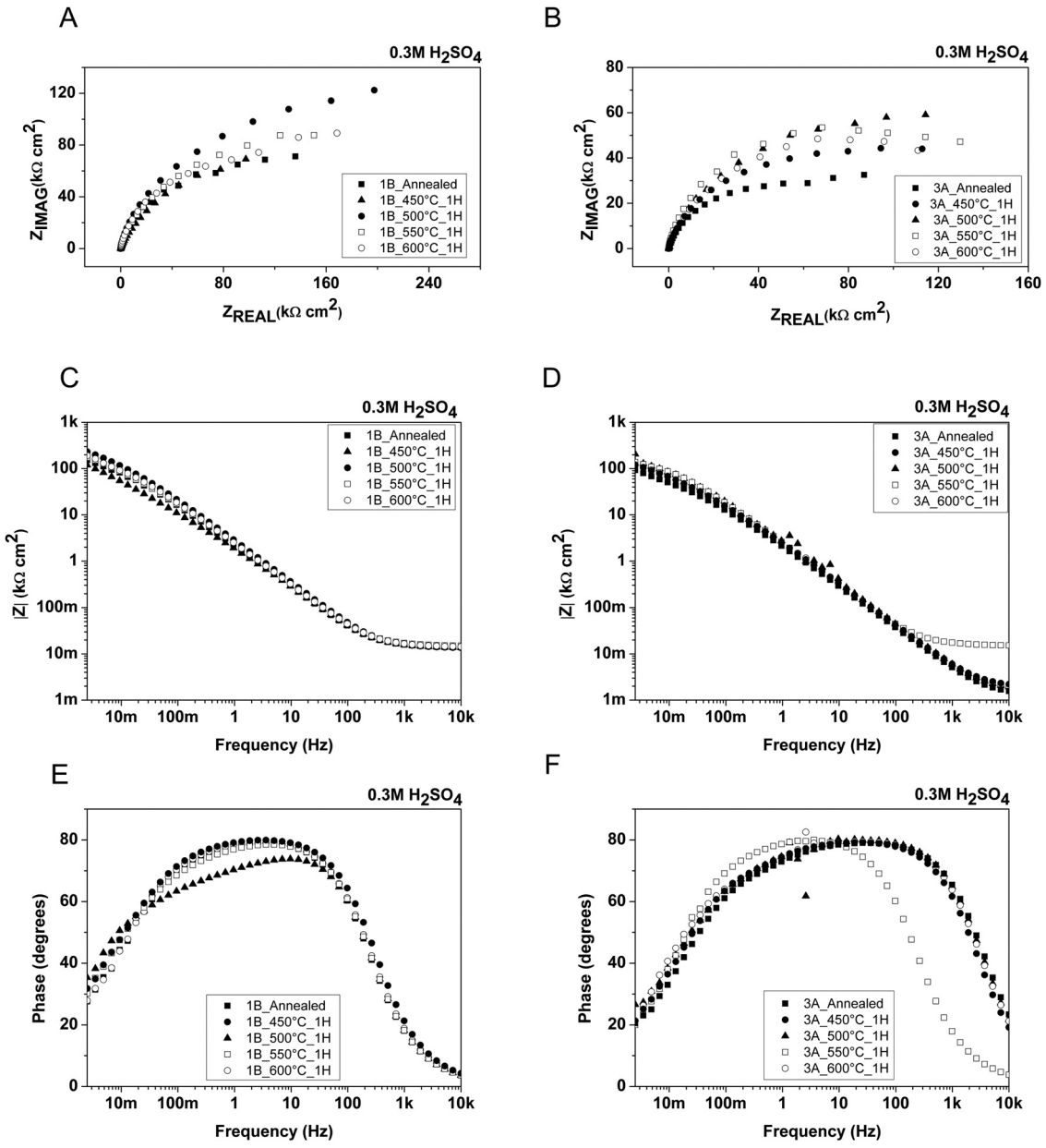

Fig. 8 – Nyquist and Bode plots for EIS data in 0.3 M H_2SO_4 of specimens (A), (C), (E) 1B and (B), (D), (F) 3A.

density achieves 100 μA cm^{-2}. Table 4 shows the CPT values obtained.

For both 1B and 3A steels, at the beginning of the test, the value for passivity current density of the annealed sample is significantly higher than that previously reported for passivity current density of stainless steel [37,38]. This effect was more pronounced for the 1B annealed sample. Similar behaviour was observed for the 3A sample aged at 600 °C. For the other samples, the current density presented a lower value during the initial heating, indicating that the DSS was well protected by the passive film. With increasing temperature, some metastable current transients, which were associated with a film breakdown process occurring in a metastable pit [39–42], were observed below the CPT. As the test temperature increased further above the CPT, the current density rose markedly due to the occurrence of stable pits.

The Cu-free samples showed the highest resistance to pitting corrosion as the CPT values of the 1B samples were lower than the CPT values of 3A samples in all conditions. This was not expected, considering that the PREN value of 3A was slightly inferior to 1B (33.9 against 35.6). These results indicate that 3.01% Cu addition is harmful to pitting corrosion resistance in 1 M NaCl.

The mechanism proposed for the reduction of CPT values for samples containing copper is that once the passive layer has been attacked locally by Cl^- anions, anodic reactions occur inside a pit or crevice, in which the pH of the solution

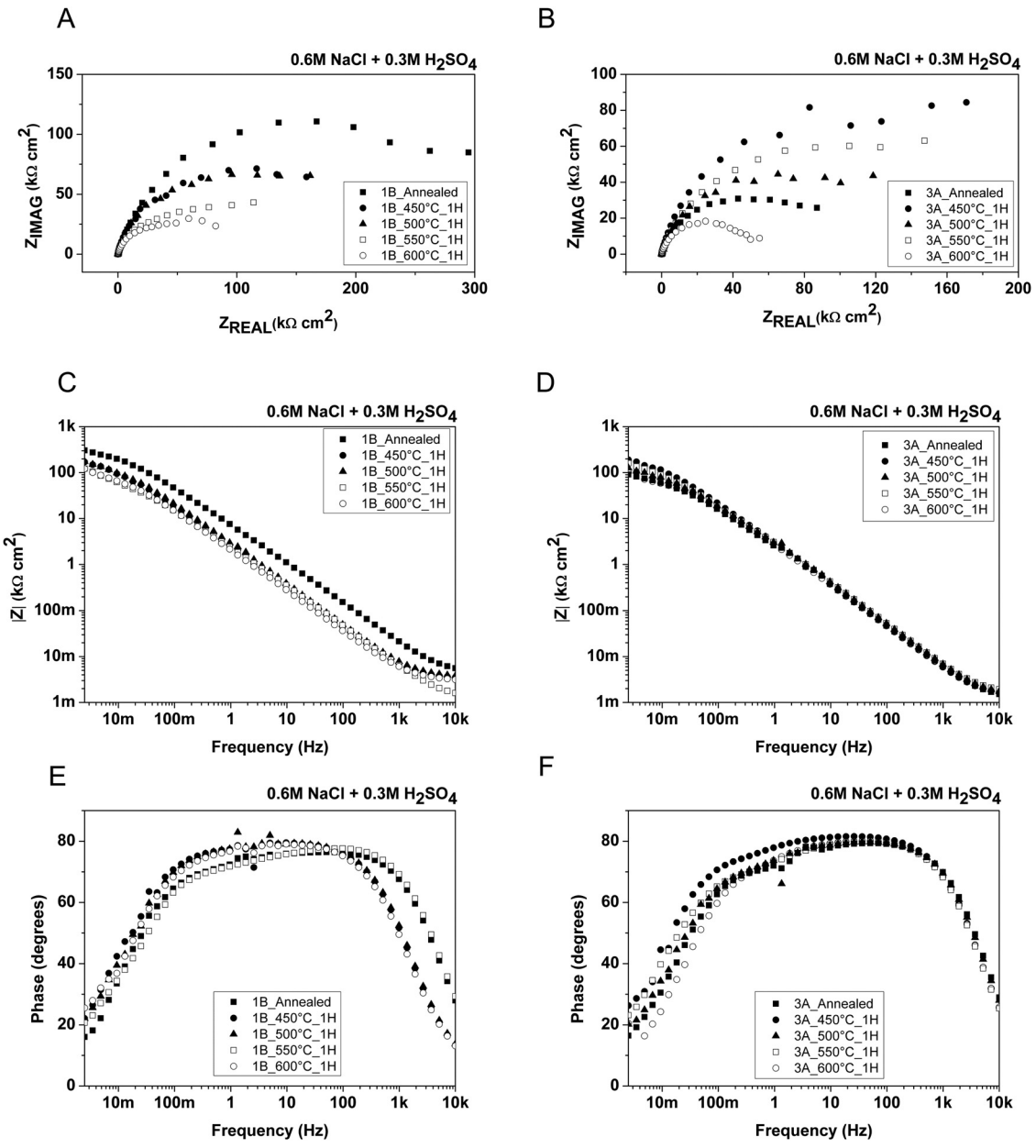

Fig. 9 – Nyquist and Bode plots for EIS data in 0.6 M NaCl + 0.3 M H_2SO_4 of specimens (A), (C), (E) 1B and (B), (D), (F) 3A.

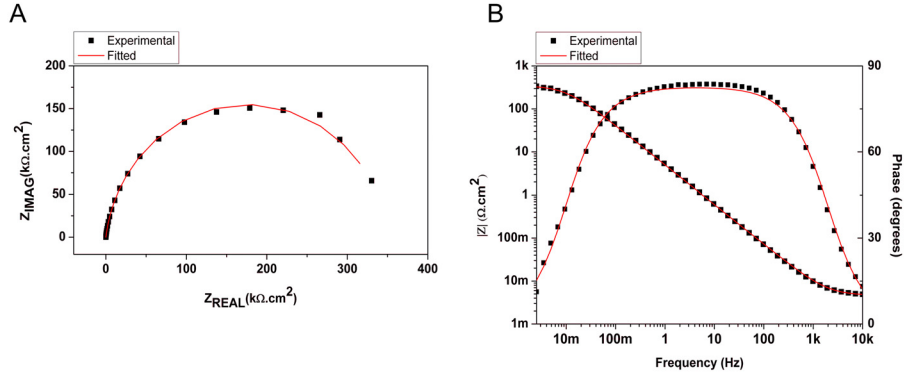

Fig. 10 – Impedance spectra for 1B DSS aged at 600 °C, experimental and fitted data: (A) Nyquist diagram and (B) Bode diagram.

Table 3 – Impedance parameters derived from the Nyquist plots of the DSSs (A) 1B and (B) 3A.

1B	0.6 M NaCl				0.3 M H_2SO_4				0.6 M NaCl + 0.3 M H_2SO_4			
	$R_s\Omega\,cm^2$	CPE		$R_{ct}k\Omega\,cm^2$	$R_s\Omega\,cm^2$	CPE		$R_{ct}k\Omega\,cm^2$	$R_s\Omega\,cm^2$	CPE		$R_{ct}k\Omega\,cm^2$
		$Y_0\mu F/cm^2$	n			$Y_0\mu F/cm^2$	n			$Y_0\mu F/cm^2$	n	
Annealed	5.25	75.62	0.995	841.80	13.49	194.34	0.996	214.02	3.06	143.27	0.996	160.03
450 °C	7.52	77.40	0.995	474.95	13.08	163.24	0.995	389.96	3.21	130.39	0.997	207.56
500 °C	4.01	67.58	0.996	943.69	13.28	277.95	0.994	229.03	3.35	130.79	0.996	217.45
550 °C	4.63	59.89	0.995	661.60	14.52	191.26	0.995	279.29	3.47	158.75	0.995	153.07
600 °C	4.64	66.82	0.998	355.10	13.92	158.65	0.995	259.16	3.42	149.69	0.996	101.69
3A	0.6 M NaCl				0.3 M H_2SO_4				0.6 M NaCl + 0.3 M H_2SO_4			
	$R_s\Omega\,cm^2$	CPE		$R_{ct}k\Omega\,cm^2$	$R_s\Omega\,cm^2$	CPE		$R_{ct}k\Omega\,cm^2$	$R_s\Omega\,cm^2$	CPE		$R_{ct}k\Omega\,cm^2$
		$Y_0\mu F/cm^2$	n			$Y_0\mu F/cm^2$	n			$Y_0\mu F/cm^2$	n	
Annealed	3.40	101.46	0.995	330.30	9.86	238.14	0.994	108.87	1.05	158.02	0.996	100.20
450 °C	4.51	68.33	0.996	437.89	16.24	168.83	0.995	160.29	1.03	131.58	0.996	204.15
500 °C	3.60	86.06	0.995	433.68	11.81	166.83	0.995	191.77	1.22	130.94	0.996	128.91
550 °C	3.89	76.23	0.997	390.82	15.03	135.83	0.997	164.02	0.90	112.80	0.995	139.61
600 °C	3.76	82.73	0.997	163.93	17.49	130.44	0.994	130.60	1.21	121.17	0.996	82.73

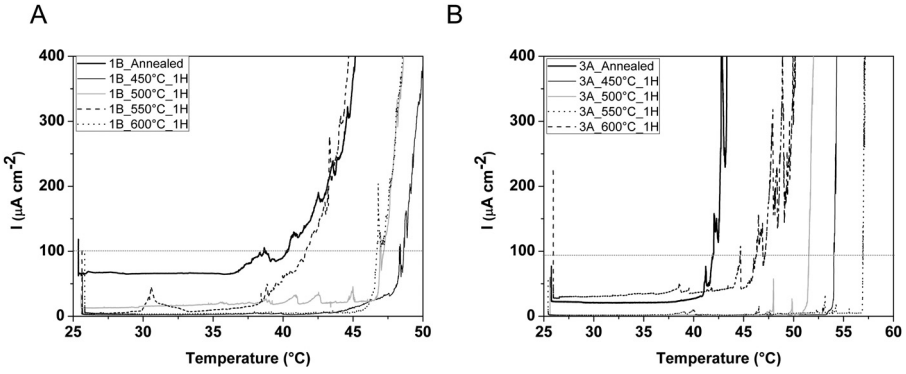

Fig. 11 – Typical curves of current density and temperature during the CPT test for DSSs (A) 1B and (B) 3A.

is low and the Cl^- concentration is high. According to the potential–pH–Cl diagram of Cu [43], depending on the potential inside a pit, Cu dissolves as $CuCl^-_2$ or deposits as metallic Cu in low pH solutions containing Cl^-. When Cu deposits, it forms a protective film, as has been reported by others [34,35]. However, the protective ability of the deposited Cu is diminished if it is unstable in a given environment, or if the amount of deposited Cu is not sufficient to protect the steel surface. Thus, judging by the results of the CPT measurements, the stability of the deposited Cu is sensitive to the temperature, being initially stable at room temperature, and then unstable when the temperature of the test increases.

It is interesting to note that ageing for 1 h in the 450–600 °C range promoted a slight increase of CPT in both steels in comparison to the annealed specimens. A similar result was observed in superduplex steel UNS S32750 aged at 400 and 475 °C, which was attributed to the redistribution of Cr, Mo and other beneficial elements by diffusion during the initial stages of ageing [44]. These treatments provoke hardening and do not decrease the pitting resistance. The effects on other properties must be investigated.

Table 4 – CPT values of DSSs steels by potentiostatic measurement in 1 M NaCl solution.

Sample	1B	3A
Annealed	40.3 ± 2	42.0 ± 2
450 °C_1 h	48.6 ± 2	54.0 ± 3
500 °C_1 h	47.2 ± 3	51.5 ± 1
550 °C_1 h	46.7 ± 3	54.9 ± 3
600 °C_1 h	41.6 ± 2	46.2 ± 2

The morphologies of specimens were observed under OM after electrochemical tests and are presented in Fig. 12. Again, the pitting corrosion was preferentially initiated in the interface between the inclusions and the metallic matrix. According to Jeon et al. [45], the increase of Cu content increased the oxide inclusions, decreasing the pitting resistance of DSSs.

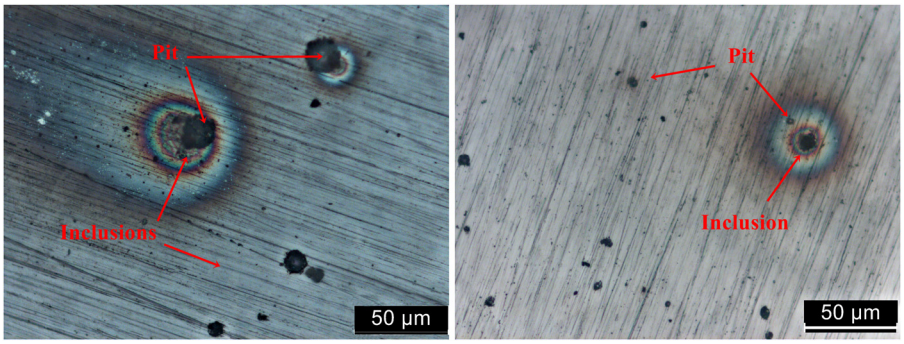

Fig. 12 – Morphologies of the corrosion attack of the material after CPT measurement: (A) pit formed on the DSS 1B aged at 550 °C, (B) pit formed on the DSS 3A aged at 550 °C.

4. Summary and conclusions

This work compared the corrosion behaviour of two cast duplex stainless steels with similar composition but different Cu contents, namely 1B (3.01% Cu) and 3A (Cu-free), both grades of ASTM A890 standard steel. The main conclusions of this comparative work are:

a) Metastable pits nucleate preferentially in the inclusions for both 1B and 3A alloys.
b) Potentiodynamic polarization results showed that: (i) polarization curves in 0.6 M NaCl display a small peak around 400 mV, still in the passivation range, which is due to metastable pits, as observed in both steels; (ii) the addition of Cu has a negative effect on the onset of passivation in 0.3 M H_2SO_4 solutions; and (iii) the increase of ageing temperature decreased the stability of the passive film formed on Cu-free samples (3A) in acidic NaCl solution.
c) Impedance results showed that Cu addition improved the charge transfer resistance (R_{ct}) in each of the media studied.
d) The CPT measurements revealed that 3.01% Cu addition is harmful to pitting corrosion resistance in chloride media.

Conflicts of interest

The authors declare no conflicts of interest.

Acknowledgments

The authors wish to acknowledge the financial support by Coordenação de Aperfeiçoamento de Pessoal de Nível Superior (Capes) and Petrobras.

REFERENCES

[1] Luo H, Dong CF, Xiao K, Li XG. Characterization of passive film on 2205 duplex stainless steel in sodium thiosulphate solution. Appl Surf Sci 2011;258:631–9.
[2] Ebrahimi N, Moayed MH, Davoodi A. Critical pitting temperature dependence of 2205 duplex stainless steel on dichromate ion concentration in chloride medium. Corros Sci 2011;53:1278–87.
[3] Yaoa YH, Weia JF, Wangb ZP. Effect of long-term thermal aging on the mechanical properties of casting duplex stainless steels. Mater Sci Eng A 2012;551:116–21.
[4] Lee S, Kuo PT, Wichman K, Chopra O. Flaw evaluation of thermally aged cast stainless steel in light-water reactor applications. Int J Press Vessel Pip 1997;72:37–44.
[5] Mburua S, Kollia RP, Pereab DE, Schwarma SC, Eatonb A, Liub J, et al. Effect of aging temperature on phase decomposition and mechanical properties in cast duplex stainless steels. Mater Sci Eng A 2017;690:365–77.
[6] Chenga X, Wangb Y, Donga C, Lia X. The beneficial galvanic effect of the constituent phases in 2205 duplex stainless steel on the passive films formed in a 3.5% NaCl solution. Corros Sci 2018;134:22–130.
[7] Olsson COA, Landolt D. Passive films on stainless steels—chemistry, structure and growth. Electrochim Acta 2003;48:1093–104.
[8] Strehblow H-H. Passivity of metals studied by surface analytical methods, a review. Electrochim Acta 2016;212:630–48.
[9] Park C-J, Know H-S. Effects of aging at 475 °C on corrosion properties of tungsten containing duplex stainless steels. Corros Sci 2002;44:2817–30.
[10] Iacoviello F, Casari F, Gianella S. Effect of "475 °C embrittlement" on duplex stainless steels localized corrosion resistance. Corros Sci 2005;47:909–22.
[11] Mateo A, Llanes L, Anglada M, Redjaimia A, Metauer G. Characterization of the intermetallic G-phase in an AISI 329 duplex stainless steel. J Mater Sci 1997;17:4533–40.
[12] Danoix F, Auger P. Atom probe studies of the Fe-Cr system and stainless steels aged at intermediate temperature: a review. Mater Charact 2000;44:177–201.
[13] Gun RN. Duplex stainless steels: microstructure, properties and applications. Mater Trans 2015;56:78–84.
[14] Jeon S-H, Kim H-J, Kong K-H, Park Y-S. Effects of copper addition on the passivity and corrosion behavior of 27Cr-7Ni hyper duplex stainless steels in sulfuric acid solution. Mater Trans 2015;56:78–84.
[15] Seo M, Hultquist G, Leygraf C, Sato N. The influence of minor alloying elements (Nb, Ti and Cu) on the corrosion resistivity of ferritic stainless steel in sulfuric acid solution. Corros Sci 1986;26:949–55.
[16] Hultquist G, Seo M, Leitner T, Leygraf C, Sato N. The dissolution behaviour of iron, chromium, molybdenum and copper from pure metals and from ferritic stainless steels. Corros Sci 1987;27:937–46.

[17] Banas J, Mazurkiewicz A. The effect of copper on passivity and corrosion behaviour of ferritic and ferritic–austenitic stainless steels. Mater Sci Eng A 2000;277:183–91.
[18] LeMay I, Schetky L. Copper in iron and steel. New York: John Wiley and Sons Inc; 1982.
[19] ASTM. A890-00 – standard specification for castings, iron–chromium–nickel–molybdenum corrosion-resistant, duplex (austenitic/ferritic) for general application. West Conshohocken, USA: ASTM; 2000.
[20] Martins M, Casteletti LC. Heat treatment temperature influence on ASTM A890 GR 6A super duplex stainless steel microstructure. Mater Charact 2005;55:225–33.
[21] ASTM. G150-99 – Standard test method for electrochemical critical pitting temperature testing of stainless steels. West Conshohocken, USA: ASTM; 2004.
[22] Chandra K, Singhal R, Kain V, Raja VS. Low temperature embrittlement of duplex stainless steel: correlation between mechanical and electrochemical behavior. Mater Sci Eng A 2010;527:3904–12.
[23] Della Rovere CA, Santos FS, Silva R, Souza CAC, Kuri SE. Influence of long-term low-temperature aging on the microhardness and corrosion properties of duplex stainless steel. Corros Sci 2013;68:84–90.
[24] Tucker JD, Miller MK, Young GA. Assessment of thermal embrittlement in duplex stainless steels 2003 and 2205 for nuclear power applications. Acta Mater 2015;87:15–24.
[25] Pareige C, Emo J, Saillet S, Domain C, Pareige P. Kinetics of G-phase precipitation and spinodal decomposition in very long aged ferrite of a Mo-free duplex stainless steel. J Nucl Mater 2015;465:383–9.
[26] Shu J, Bi H, Li X, Xu Z. The effect of copper and molybdenum on pitting corrosion and stress corrosion cracking behavior of ultra-pure ferritic stainless steels. Corros Sci 2012;57:89–98.
[27] Tavares SSM, Pardal JM, Almeida BB, Mendes MT, Freire JLF, Vidal AC. Failure of superduplex stainless steel flange due to inadequate microstructure and fabrication process. Eng Fail Anal 2018;84:1–10.
[28] Fattah-alhosseini A, Vafaeian S. Comparison of electrochemical behavior between coarse-grained and fine-grained AISI 430 ferritic stainless steel by Mott–Schottky analysis and EIS measurements. J Alloys Comp 2015;639:301–7.
[29] Oguzie EE, Li J, Liu Y, Chen D, Li Y, Yang K, et al. The effect of Cu addition on the electrochemical corrosion and passivation behavior of stainless steel. Electrochim Acta 2010;55:5028–35.
[30] Qiu JH. Passivity and its breakdown on stainless steels and alloys. Surf Inter Anal 2002;33:830–3.
[31] Zheng ZB, Zheng YG, Sun WH, Wang JQ. Effect of applied potential on passivation and erosion–corrosion of a Fe-based amorphous metallic coating under slurry impingement. Corros Sci 2014;82:115–24.
[32] Alonso-Falleiros N, Hakim A, Wolynec S. Comparison between potentiodynamic and potentiostatic tests for pitting potential measurement of duplex stainless steels. Corrosion 1999;55:443–8.
[33] Fernandez-Domene RM, Blasco-Tamarit E, Garcia-Garcia DM, Garcia-Anton J. Passive and transpassive behaviour of Alloy 31 in a heavy brine LiBr solution. Electrochim Acta 2013;95:1–11.
[34] Pardo A, Merino MC, Carboneras M, Coy AE, Arrabal R. Pitting corrosion behaviour of austenitic stainless steels with Cu and Sn additions. Corros Sci 2007;49:510–25.
[35] Oguzie EE, Li J, Liu Y, Chen D, Li Y, Yang K, et al. Electrochemical corrosion behavior of novel Cu-containing antimicrobial austenitic and ferritic stainless steels in chloride media. J Mater Sci 2010;45:5902–9.
[36] Zhao J, Dake X, Shahzad MB, Kang Q, Sun Y, Sun Z, et al. Effect of surface passivation on corrosion resistance and antibacterial properties of Cu-bearing 316L stainless steel. Appl Surf Sci 2016;386:371–80.
[37] Burstein GT, Pistorius PC, Mattin SP. The nucleation and growth of corrosion pits on stainless steel. Corros Sci 1993;35:57–62.
[38] Ebrahimi N, Momeni M, Kosari A, Zakeri M, Moayed MH. A comparative study of critical pitting temperature (CPT) of stainless steels by electrochemical impedance spectroscopy (EIS), potentiodynamic and potentiostatic techniques. Corros Sci 2012;59:96–102.
[39] Burstein GT, Daymond BT. The remarkable passivity of austenitic stainless steel in sulphuric acid solution and the effect of repetitive temperature cycling. Corros Sci 2009;51:2249–52.
[40] Deng B, Wang Z, Jiang Y, Sun T, Xu J, Li J. Effect of thermal cycles on the corrosion and mechanical properties of UNS S31803 duplex stainless steel. Corros Sci 2009;51:2969–75.
[41] Mesias LFG, Sykes JM. Metastable pitting in 25Cr duplex stainless steel. Corros Sci 1999;41:959–87.
[42] Moayed MH, Newman RC. Evolution of current transients and morphology of metastable and stable pitting on stainless steel near the critical pitting temperature. Corros Sci 2006;48:1004–18.
[43] Ujiro T, Satoh S, Staehle RW, Smyrl WH. Effect of alloying Cu on the corrosion resistance of stainless steels in chloride media. Corros Sci 2001;43:2185–200.
[44] Tavares SSM, Loureiro A, Pardal JM, Montenegro TR, Costa VC. Influence of heat treatments at 475 and 400 °C on the pitting corrosion resistance and sensitization of UNS S32750 and UNS S32760 superduplex stainless steels. Mater Corros 2011;62:1–5.
[45] Jeon S-H, Kim S-T, Lee I-S, Park J-H, Kim K-T, Kim J-S, et al. Effects of copper addition on the formation of inclusions and the resistance to pitting corrosion of high performance duplex stainless steels. Corros Sci 2011;53:1408–16.